JACS
JOURNAL OF THE AMERICAN CHEMICAL SOCIETY
pubs.acs.org/JACS

Communication

Photodriven Sm(III)-to-Sm(II) Reduction for Catalytic Applications

Christian M. Johansen,[‡] Emily A. Boyd,[‡] Drew E. Tarnopol, and Jonas C. Peters*

Cite This: J. Am. Chem. Soc. 2024, 146, 25456−25461

ABSTRACT: The selectivity of SmI_2 as a one electron-reductant motivates the development of methods for reductive Sm-catalysis. Photochemical methods for SmI_2 regeneration are desired for catalytic transformations. In particular, returning Sm^{III}-alkoxides to Sm^{II} is a crucial step for Sm-turnover in many potential applications. To this end, photochemical conditions for reduction of both SmI_3 and a model Sm^{III}-alkoxide to $SmI_2(THF)_n$ are described here. The Hantzsch ester can serve either as a direct photoreductant or as the reductive quencher for an Ir-based photoredox catalyst. In contrast to previous Sm^{III} reduction methodologies, no Lewis acidic additives or byproducts are involved, facilitating selective ligand coordination to Sm. Accordingly, Sm^{II} species can be generated photochemically from SmI_3 in the presence of protic, chiral, and/or Lewis basic additives. Both the photoreductant and photoredox methods for SmI_2 generation translate to intermolecular ketone-acrylate coupling as a proof-of-concept demonstration of a photodriven, Sm-catalyzed reductive cross-coupling reaction.

Samarium diiodide (SmI_2) is an exceptionally versatile single-electron reductant. The large and labile coordination sphere of Sm^{II} can recruit one or multiple substrates and additives to achieve selectivity in both organic synthesis and small-molecule reductions (Figure 1A).[1−4] However, SmI_2 is employed stoichiometrically in all but a few select cases[5−8] because its reactions typically terminate in the formation of highly stable Sm^{III}−alkoxide species. Catalytic regeneration of the Sm^{II} state requires abstraction of OR^- by a stoichiometric oxophile (EX) to generate a Sm^{III} species that can be reduced by a relatively mild reductant (Figure 1A). The difficulty associated with this transformation has been cited as a motivation for the development of a variety of alternative photo- and electrochemically driven methods for ketyl radical generation.[9−13]

Early strategies for reductive Sm catalysis relied on harsh combinations of halosilane oxophiles (R_3SiX) and low valent metals (Mg^0 for X = Cl; Zn^0 for X = I) or an applied electrochemical potential as the reductant.[14−22] In a collaborative effort with the Reisman laboratory, we recently disclosed comparatively mild silane-free thermal and electrochemical conditions for catalytic turnover of SmI_2 in reductive coupling of ketones and acrylates through combination of cationic Brønsted acids with either Zn^0 or an applied potential of −1.55 V vs $Fc^{+/0}$ ($Fc^{+/0}$ = ferrocenium/ferrocene; all potentials referenced to $Fc^{+/0}$).[23]

Given the growing interest in (metalla)photoredox catalysis,[24] photodriven strategies for $Ln^{III/II}$ catalysis remain surprisingly underexplored.[25,26] In a strategy recently showcased by the groups of Borbas[27] and Nemoto,[28] photosensitizers are incorporated into the secondary coordination spheres of Ln^{III} complexes (Ln = Sm, Eu; Figure 1B). Intramolecular oxidative quenching of the excited sensitizer by the Ln^{III} center produces a potent Ln^{II} reductant which can carry out a variety of transformations.

While this and other strategies show promise,[25−28] the chelating ligand platforms used thus far in photodriven $Ln^{III/II}$ catalysis (cryptands, bidentate phosphine oxides) restrict the coordination sphere and/or shift $E°(Ln^{III/II})$ to strongly negative potentials, belying direct translation to the rich stoichiometric chemistry of $SmI_2(L)_n$ as an inner sphere reductant (L = solvent molecule, typically THF).

Lewis acidic metal ions are commonly used to template substrates in photodriven reductive coupling reactions.[10,29,30] Recently, in contrast to the use of photocatalysts, several Lewis acid-mediated photoreductions utilize the blue-light absorbing Hantzsch ester (HEH_2) as a photoreductant ($E(HEH_2^{+\bullet}/{}^*HEH_2)$ = −2.5 V).[31−34] Photoexcited HEH_2 ($^*HEH_2$) carries out Cr^{III} reduction in a catalytic-in-Cr photodriven Nozaki−Hiyama−Kishi reaction (Figure 1C).[35] Alternatively, HEH_2 acts as a photoreductant in a $Gd(OTf)_3$-mediated Giese addition of an *N*-hydroxyphthalimide (NHPI) ester-derived alkyl radical into α,β-unsaturated ketones or a lactone (Figure 1C).[36] In the latter study, an interaction between Gd and HEH_2 is observed, but Gd^{III} reduction to Gd^{II} is not accessible even by $^*HEH_2$.[23]

Based on these precedents we noted that $^*HEH_2$ should be capable of reducing Sm^{III}-species such as SmI_3 ($E°(SmI_3/(SmI_2 + I^-))$ = −1.58 V; Figure S35). Because Sm and Gd are similar in size and oxophilicity, we envisioned that photoexcitation of HEH_2 bound to Sm^{III} could result in intramolecular oxidative quenching to produce Sm^{II} (Figure 1D). Crucially, however, a more dynamic Sm-chromophore interaction might allow access to coordinatively unsaturated

Received: July 23, 2024
Revised: August 23, 2024
Accepted: August 26, 2024
Published: September 3, 2024

https://doi.org/10.1021/jacs.4c10053
J. Am. Chem. Soc. 2024, 146, 25456−25461

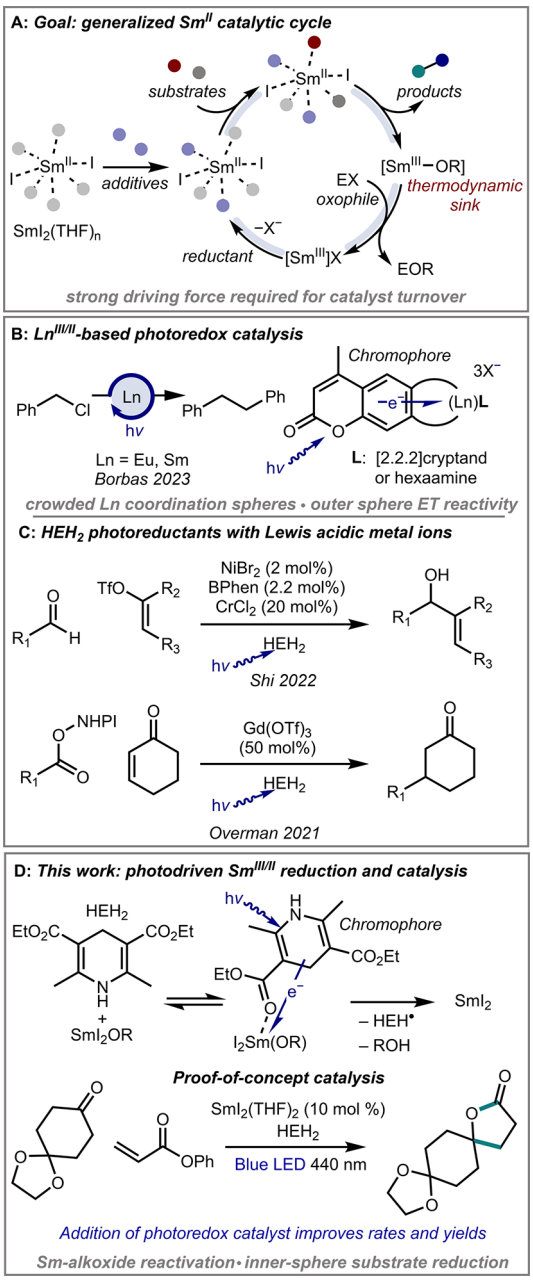

Figure 1. Summary of key challenges for Sm-turnover; prior studies exploiting $Ln^{III/II}$ photochemistry and photoreductions with HEH_2 and Lewis acidic metals; and this work describing photodriven generation of SmI_2.

$SmI_2(L)_n$ species which could carry out inner-sphere reduction in a photodriven Sm-catalyzed cross-coupling reaction. Importantly, both HEH_2 and its $2H^+/2e^-$ oxidized congener, HE, are weak bases and are therefore compatible with the acidic conditions necessary for recovery of inactive Sm^{III}–OR species by protonolysis.

Gratifyingly, HEH_2 proved competent as a photoreductant for Sm^{III}-to-Sm^{II} conversion. Monitoring the UV–visible absorption spectrum of a solution of SmI_3 (2 mM), HEH_2 (60 mM) and 2,6-lutidine base (Lut, 60 mM) following irradiation at 440 nm for 5 min in THF reveals the characteristic profile of blue $SmI_2(THF)_n$ with λ_{max} at 555 and 618 nm (Figure 2A, left panel). Extended irradiation (120 min) results in increasing SmI_2 generation, with maximum

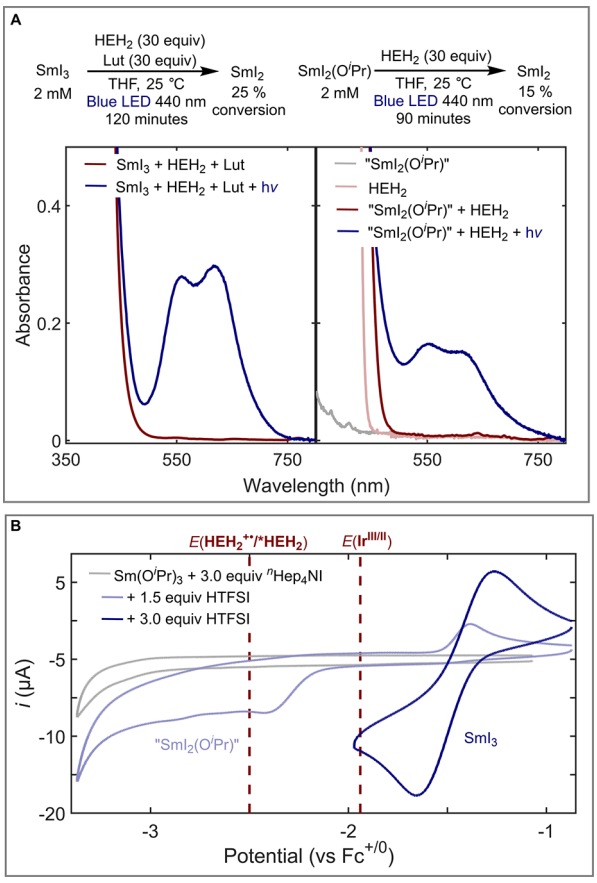

Figure 2. (A) UV–vis spectra following photoreduction of SmI_3 (left) and $SmI_2(O^iPr)(L)_n$ to form SmI_2. CVs of $Sm(O^iPr)_3$ (2 mM) in the presence of iodide and proton sources in THF.

yield ~25%. Interestingly, in the absence of base this reaction does not proceed (Figure S17), likely due to rapid back-electron transfer (BET) between $HEH_2^{\bullet+}$ and SmI_2. However, $HEH_2^{\bullet+}$ can be deprotonated in the presence of base, circumventing BET.

We next evaluated conditions for photogeneration of $SmI_2(THF)_n$ from $Sm(O^iPr)_3$ as a model Sm^{III}-alkoxide. Irradiation of $Sm(O^iPr)_3$ (2 mM), tetra-*n*-heptylammonium iodide ($^nHep_4NI$, 6 mM), and HEH_2 (60 mM) at 440 nm in THF shows no evidence of SmI_2 formation (Figure S19). However, upon the addition of only 1.5 equiv of the acid *bis*-trifluoromethylsulfonylimide (HTFSI) to $Sm(O^iPr)_3$, $SmI_2(THF)_n$ is generated upon irradiation with $^nHep_4NI$ and HEH_2 (Figure 2A, right panel). Parallel CV studies demonstrate that no SmI_3 is generated from $Sm(O^iPr)_3$ at this acid loading (Figure 2B, compare light and dark blue traces), and current attributable to Sm^{III} reduction (presumably of an intermediate mixture of solvated "$SmI(O^iPr)_2$" and "SmI_2O^iPr") does not onset until −2.3 V. In contrast to SmI_3, no external base is needed, suggesting that the Sm-bound alkoxide might additionally serve the role of deprotonating $HEH_2^{\bullet+}$ to avoid BET. UV–vis studies reveal that addition of the colorless Sm^{III}–O^iPr species (gray trace in Figure 2A) gives rise to a significantly red-shifted shoulder in the HEH_2 absorption profile (compare light and dark red traces in Figure 2A), consistent with preassociation.

The modest yields and rates of these reactions motivated the study of Sm^{III} reduction with a photoredox catalyst to

https://doi.org/10.1021/jacs.4c10053
J. Am. Chem. Soc. 2024, 146, 25456–25461

overcome the low quantum yield and excited state lifetime (220 ps in MeCN)[37] of HEH_2.

We selected $[Ir(dtbbpy)(ppy)_2]^+$ ($[\mathbf{Ir^{III}}]^+$)[38] as a photosensitizer, which could undergo reductive quenching by a sacrificial electron donor to generate $\mathbf{Ir^{II}}$. $\mathbf{Ir^{II}}$ is thermodynamically capable of reducing SmI_3 to SmI_2 ($E^\circ(\mathbf{Ir^{III/II}}) = -1.94$ V, Figure 2B and Figure S36).

Irradiating SmI_3 or SmI_2O^iPr (2 mM) with $[\mathbf{Ir^{III}}]PF_6$ (0.2 mM), HEH_2 (60 mM) as sacrificial reductant, and Lut (60 mM) rapidly generates SmI_2 (80% or 30% conversion in 2 min, Figure 3A). Again, the weak base Lut enhances the process (Figures S20–S21).

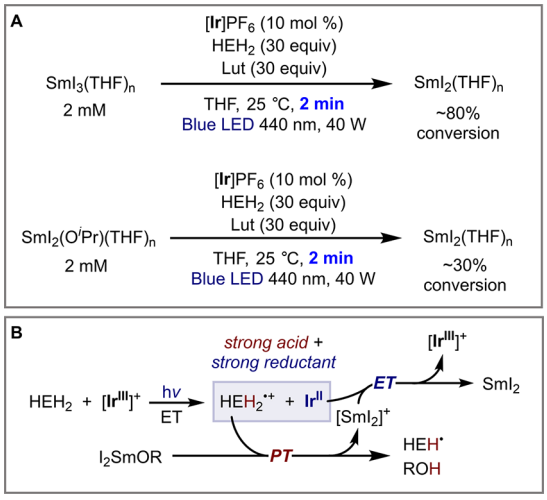

Figure 3. (A) Photoreductions of Sm^{III} species with $[\mathbf{Ir}]PF_6$ photocatalyst. (B) Rationale for net photoinduced proton- and electron-transfer from HEH_2 to $[Sm^{III}–OR]$ species.

The accelerated reduction of SmI_2O^iPr is curious, as electron transfer from $\mathbf{Ir^{II}}$ to this Sm^{III} species is uphill by 400 mV (Figure 2B). A rationale for these observations is provided in Figure 3B: reductive quenching of $*[\mathbf{Ir^{III}}]^+$ by HEH_2 generates not only the strong reductant $\mathbf{Ir^{II}}$, but also the strong acid $HEH_2^{\bullet+}$ ($pK_a - 1$ in MeCN),[39,40] the combination of which can carry out net proton-coupled electron transfer to $Sm^{III}–O^iPr$.[41] Proton transfer from $HEH_2^{\bullet+}$ to a $Sm^{III}–O^iPr$ species, likely via proton relay mediated by Lut, liberates ^{i}PrOH and $[SmI_2]^+$.[42] The latter can then be reduced to SmI_2 by $\mathbf{Ir^{II}}$.

Development of Sm-catalysis leveraging diverse ligand coordination to modulate reactivity is an attractive goal. Exploration of Sm^{II} generation in the presence of potential coligands was carried out pursuant to these interests.

Satisfyingly, Sm^{II} is readily photogenerated from SmI_3 by $[\mathbf{Ir^{III}}]^+$ and quencher (HEH_2 or Et_3N) in the presence of several protic additives (ethylene glycol, *N*,*N*-dimethylaminoethanol, Figures S23–S24),[3,43–45] including a chiral aminediol (Figure 4A, Figure S25) that has been utilized in several enantioselective SmI_2 transformations.[46–48]

The reduction potential and reactivity of Sm^{II} is highly sensitive to coordination of Lewis-basic additives (HMPA, Br^-; Figure 4A).[49] While $[\mathbf{Ir^{II}}]$ is insufficiently reducing to access such species, the more reducing photocatalyst 3DPA2FBN,[50] when paired with the more reducing quencher 9,10-dihydroacridine and Et_3N as base, mediates generation of both $SmBr_2$ and $Sm(HMPA)_4^{2+}$ (Figure 4B). 3DPA2FBN also

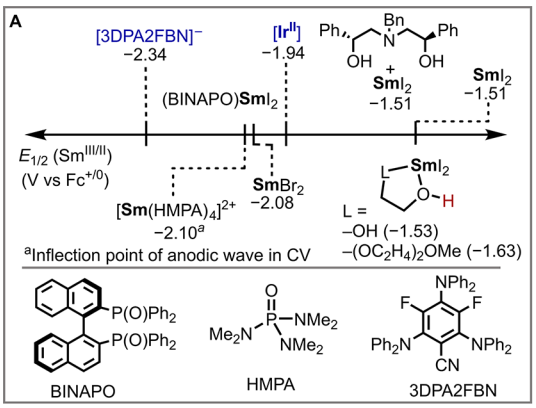

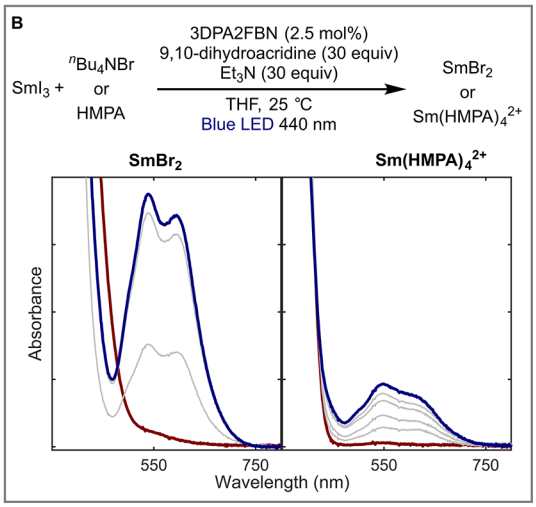

Figure 4. (A) Ligand coordinated Sm-species generated by a photoredox approach. See SI for relevant electrochemical data. Choice of a sufficiently reducing photocatalyst remains crucial to observe Sm^{II}. (B) UV–vis spectra following photogeneration of $SmBr_2$ and $Sm(HMPA)_4^{2+}$.

facilitates Sm^{III} reduction and binding to the chiral BINAPO ligand (Figures 4A and S34).[51,52]

Having established two different photochemical approaches to Sm^{II} generation, we targeted an intermolecular ketone-acrylate coupling as a model reaction to benchmark photo-driven Sm-catalysis (Table 1). This reaction is representative of the qualities that set SmI_2 apart as a stoichiometric reductant. Inner-sphere electron transfer to one or both of the carbonyl substrates is obligatory based on comparison of outer-sphere reduction potentials.[23] Importantly, a Sm-alkoxide is generated as the byproduct of lactonization, enabling evaluation of the ability of a set of conditions to overcome this critical barrier to generalizable Sm catalysis.

Irradiation of ketone **1** (0.04 mmol), phenyl acrylate (2 equiv), and $SmI_2(THF)_2$ (10 mol %) in the presence of HEH_2 (4.0 equiv) in 2-MeTHF (0.02 M) at 440 nm for 90 min yields lactone **2** in 76% yield (Table 1, entry 1, method A). Addition of a photoredox catalyst ($[\mathbf{Ir}]PF_6$, 1 mol %) with pyridine (2 equiv) results in an increase in yield to 89% (entry 1, method B). Light and Sm were required for catalytic formation of **2** by either method (entries 3 and 4). $Sm(OTf)_3$ is a competent precatalyst with 50 mol % MgI_2 included as an iodide source (entry 4). Substitution of $Gd(OTf)_3$ for $Sm(OTf)_3$ results in trace product formation, supporting a key role for Sm^{II} in catalysis (entry 5).

https://doi.org/10.1021/jacs.4c10053
J. Am. Chem. Soc. 2024, 146, 25456–25461

Table 1. Photodriven Sm-Catalyzed Coupling of Ketones and Phenyl Acrylate to Form Lactone Products[a]

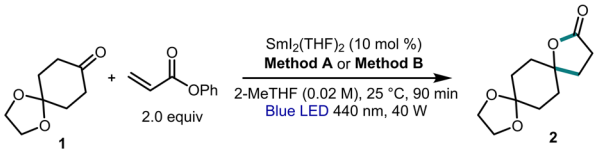

Method A: HEH_2 (4 equiv)
Method B: HEH_2 (4 equiv), [**Ir**]PF_6 (1 mol %) and pyridine (2 equiv)

Entry	Deviation	Yield (%) Method A	Yield (%) Method B
1	None	76	89
2	No Irradiation	4	4
3	No Sm	0	0
4	10 mol% $Sm(OTf)_3$ / 50 mol % MgI_2 instead of SmI_2	60	85
5	10 mol% $Gd(OTf)_3$ / 50 mol % MgI_2 instead of SmI_2	0	6
6	2 equiv pyridine added	72	–
7	No pyridine	–	82
8	2 equiv Et_3N added (A)/instead of pyridine (B)	5	15
9	5,6-dihydrophenanthridine instead of HEH_2	0	77
10	15 min	29	60
11	Ethyl acrylate instead of phenyl acrylate	31	58

Entry	12	13	14	15[b]
Product	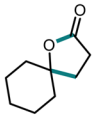	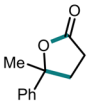	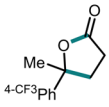	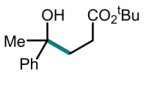
	3	4	5	6
Method A:	32%	<95%	77%	43%
Method B:	77%	90%	49%	29%

[a]Yields were determined by ^1H NMR analysis. For additional reaction data, see Table S2. [b]*tert*-Butyl acrylate used as coupling partner; lactonization observed only upon acidic workup.

Both methods are competent in the presence/absence of pyridine (entries 1, 6, and 7), but yields are greatly diminished in the presence of a stronger base (Et_3N, entry 8). This suggests that the dynamics of Sm-alkoxide protonation play an important role in turnover.[23] Interestingly, the use of a dihydropyridine without carbonyl groups, 5,6-dihydrophenanthridine, only shows product formation with [**Ir**]$^+$ (entry 9). In the absence of Ir, the specific interaction between Sm and HEH_2 appears to be required. The Ir-catalyzed reaction is also faster, achieving 60% conversion in 15 min, compared to 29% by method A (entry 10).

Methods A and B were tested against alternative coupling partners to assess their relative efficacies. When using less activated substrate pairs (aliphatic ketones and alkyl acrylates, entries 1, 11 and 12), method B is favored, perhaps because these slower cross-couplings require rapid Sm^{III}-to-Sm^{II} conversion. Method A is preferred when using aryl ketones (entries 13−15), as method B gives considerable pinacol-coupled side-products (Table S3). With method A, selective inner-sphere photogeneration of Sm^{II} by Sm^{III}−HEH_2 may favor Sm^{II}-mediated cross-coupling, while with method B background Ir-mediated substrate reduction to homocoupled products can dominate.

A proposed mechanism for this photodriven lactonization reaction (by method A) is presented in Figure 5. The mechanism can be divided into two parts, a photoreduction side in which Sm^{III} is reduced to Sm^{II}, and a SmI_2 cross-coupling side where the organic substrates are coupled. Starting from $SmI_2(OPh)$, coordination to HEH_2 (as

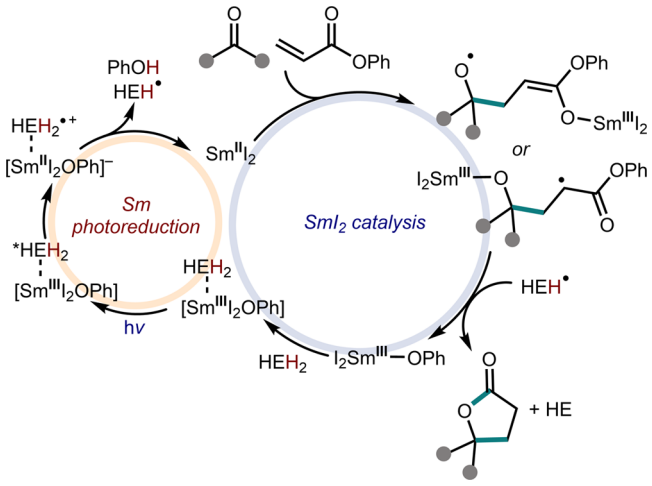

Figure 5. Proposed mechanism of Sm cross-coupling under Ir-free conditions (method A).

demonstrated in Figure 2A) followed by excitation to $*HEH_2$ allows for the proton and electron transfer required to generate SmI_2, with PhOH and HEH$^\bullet$ as additional products. Subsequently, SmI_2 couples the acrylate and ketone to form a radical intermediate.[53,54] HEH$^\bullet$ is capable of reducing this intermediate as a potent H atom donor, although alternative schemes for reduction of the radical intermediate can be envisioned (Figure S45). Following reduction and lactonization, **2** is formed along with $SmI_2(OPh)$.

With [**Ir**]$^+$, a similar mechanism is proposed, differing in the regeneration of Sm^{II}, which can be regenerated from Sm^{III}-alkoxide as depicted in Figure 3B (see Figure S46 for full scheme).

In summary, we have demonstrated photodriven generation of $SmI_2(THF)_2$ from Sm^{III} precursors using both a photoreductant and a photoredox catalyst. These conditions translate to proof-of-concept photodriven reductive Sm-catalyzed ketone-acrylate coupling. Distinct from reported methods, photodriven Sm-catalysis occurs in the absence of competing Lewis-acidic metal additives and byproducts (e.g., Mg^{2+} and Zn^{2+} salts),[14−23] which may be of utility in development of Sm-catalysis with ligands.[3,18,43,46−51] These findings are anticipated to facilitate applications of Sm-catalysis beyond the types of thermally driven transformations studied thus far.

■ ASSOCIATED CONTENT

Supporting Information

The Supporting Information is available free of charge at https://pubs.acs.org/doi/10.1021/jacs.4c10053.

Experimental methods, data from individual catalysis experiments, and additional spectra as referenced in the text. (PDF)

■ AUTHOR INFORMATION

Corresponding Author

Jonas C. Peters − *Division of Chemistry and Chemical Engineering, California Institute of Technology (Caltech), Pasadena, California 91125, United States;* orcid.org/0000-0002-6610-4414; Email: jpeters@caltech.edu

https://doi.org/10.1021/jacs.4c10053
J. Am. Chem. Soc. 2024, 146, 25456−25461

Authors

Christian M. Johansen − *Division of Chemistry and Chemical Engineering, California Institute of Technology (Caltech), Pasadena, California 91125, United States;* orcid.org/0000-0003-0066-4424

Emily A. Boyd − *Division of Chemistry and Chemical Engineering, California Institute of Technology (Caltech), Pasadena, California 91125, United States;* orcid.org/0000-0003-0150-5396

Drew E. Tarnopol − *Division of Chemistry and Chemical Engineering, California Institute of Technology (Caltech), Pasadena, California 91125, United States*

Complete contact information is available at: https://pubs.acs.org/10.1021/jacs.4c10053

Author Contributions

‡C.M.J. and E.A.B. contributed equally.

Notes

The authors declare no competing financial interest.

■ ACKNOWLEDGMENTS

We thank the National Institutes of Health (R35GM153322). E.A.B. and D.E.T. thank the National Science Foundation for a Graduate Research Fellowship under Grant No. DGE-1745301 and 2139433, respectively. C.M.J. is grateful for support from the Aker Scholarship foundation. We also acknowledge the Resnick Sustainability Institute at Caltech for support of enabling facilities. We thank the Reisman laboratory for supplying ligand samples.

■ REFERENCES

(1) Girard, P.; Namy, J. L.; Kagan, H. B. Divalent Lanthanide Derivatives in Organic Synthesis. 1. Mild Preparation of Samarium Iodide and Ytterbium Iodide and Their Use as Reducing or Coupling Agents. *J. Am. Chem. Soc.* **1980**, *102* (8), 2693−2698.

(2) Szostak, M.; Fazakerley, N. J.; Parmar, D.; Procter, D. J. Cross-Coupling Reactions Using Samarium(II) Iodide. *Chem. Rev.* **2014**, *114* (11), 5959−6039.

(3) Ashida, Y.; Arashiba, K.; Nakajima, K.; Nishibayashi, Y. Molybdenum-catalysed Ammonia Production with Samarium Diiodide and Alcohols or Water. *Nature* **2019**, *568* (7753), 536−540.

(4) Lee, C. C.; Hu, Y.; Ribbe, M. W. Catalytic Reduction of CN^-, CO, and CO_2 by Nitrogenase Cofactors in Lanthanide-Driven Reactions. *Angew. Chem., Int. Ed.* **2015**, *54* (4), 1219−1222.

(5) Net redox-neutral SmI_2-catalyzed radical relay processes have been explored; see the following and refs 6−8: Huang, H.-M.; McDouall, J. J. W.; Procter, D. J. SmI_2-Catalysed Cyclization Cascades by Radical Relay. *Nat. Catal.* **2019**, *2* (3), 211−218.

(6) Agasti, S.; Beattie, N. A.; McDouall, J. J. W.; Procter, D. J. SmI_2-Catalyzed Intermolecular Coupling of Cyclopropyl Ketones and Alkynes: A Link between Ketone Conformation and Reactivity. *J. Am. Chem. Soc.* **2021**, *143* (9), 3655−3661.

(7) Agasti, S.; Beltran, F.; Pye, E.; Kaltsoyannis, N.; Crisenza, G. E. M.; Procter, D. J. A Catalytic Alkene Insertion Approach to Bicyclo[2.1.1]hexane Bioisosteres. *Nat. Chem.* **2023**, *15* (4), 535−541.

(8) Mansell, J. I.; Yu, S.; Li, M.; Pye, E.; Yin, C.; Beltran, F.; Rossi-Ashton, J. A.; Romano, C.; Kaltsoyannis, N.; Procter, D. J. Alkyl Cyclopropyl Ketones in Catalytic Formal [3 + 2] Cycloadditions: The Role of SmI_2 Catalyst Stabilization. *J. Am. Chem. Soc.* **2024**, *146* (18), 12799−12807.

(9) Edgecomb, J. M.; Alektiar, S. N.; Cowper, N. G. W.; Sowin, J. A.; Wickens, Z. K. Ketyl Radical Coupling Enabled by Polycyclic Aromatic Hydrocarbon Electrophotocatalysts. *J. Am. Chem. Soc.* **2023**, *145* (37), 20169−20175.

(10) Lee, K. N.; Lei, Z.; Ngai, M.-Y. *β*-Selective Reductive Coupling of Alkenylpyridines with Aldehydes and Imines via Synergistic Lewis Acid/Photoredox Catalysis. *J. Am. Chem. Soc.* **2017**, *139* (14), 5003−5006.

(11) Derosa, J.; Garrido-Barros, P.; Peters, J. C. Electrocatalytic Ketyl-Olefin Cyclization at a Favorable Applied Bias Enabled by a Concerted Proton-Electron Transfer Mediator. *Inorg. Chem.* **2022**, *61* (17), 6672−6678.

(12) Tarantino, K. T.; Liu, P.; Knowles, R. R. Catalytic Ketyl-Olefin Cyclizations Enabled by Proton-Coupled Electron Transfer. *J. Am. Chem. Soc.* **2013**, *135* (27), 10022−10025.

(13) Seo, H.; Jamison, T. F. Catalytic Generation and Use of Ketyl Radical from Unactivated Aliphatic Carbonyl Compounds. *Org. Lett.* **2019**, *21* (24), 10159−10163.

(14) Corey, E. J.; Zheng, G. Z. Catalytic Reactions of Samarium (II) Iodide. *Tetrahedron Lett.* **1997**, *38* (12), 2045−2048.

(15) Nomura, R.; Matsuno, T.; Endo, T. Samarium Iodide-Catalyzed Pinacol Coupling of Carbonyl Compounds. *J. Am. Chem. Soc.* **1996**, *118* (46), 11666−11667.

(16) Aspinall, H. C.; Greeves, N.; Valla, C. Samarium Diiodide-Catalyzed Diastereoselective Pinacol Couplings. *Org. Lett.* **2005**, *7* (10), 1919−1922.

(17) Sun, L.; Sahloul, K.; Mellah, M. Use of Electrochemistry to Provide Efficient SmI_2 Catalytic System for Coupling Reactions. *ACS Catal.* **2013**, *3* (11), 2568−2573.

(18) Maity, S.; Flowers, R. A. Mechanistic Study and Development of Catalytic Reactions of Sm(II). *J. Am. Chem. Soc.* **2019**, *141* (7), 3207−3216.

(19) Hébri, H.; Duñach, E.; Heintz, M.; Troupel, M.; Périchon, J. Samarium-Catalyzed Electrosynthesis of 1,2-Diketones by the Direct Reductive Dimerization of Aromatic Esters: A Novel Coupling Reaction. *Synlett* **1991**, *1991* (12), 901−902.

(20) Hebri, H.; Duñach, E.; Périchon, J. $SmCl_3$-Catalysed Electrosynthesis of *γ*-Butyrolactones from 3-Chloroesters and Carbonyl Compounds. *J. Chem. Soc., Chem. Commun.* **1993**, *6*, 499−500.

(21) Hebri, H.; Duñach, E.; Périchon, J. Samarium-Catalyzed Electrochemical Reduction of Organic Halides. *Synth. Commun.* **1991**, *21* (22), 2377−2382.

(22) Espanet, B.; Duñach, E.; Périchon, J. $SmCl_3$-Catalyzed Electrochemical Cleavage of Allyl Ethers. *Tetrahedron Lett.* **1992**, *33* (18), 2485−2488.

(23) Boyd, E. A.; Shin, C.; Charboneau, D. J.; Peters, J. C.; Reisman, S. E. Reductive Samarium (Electro)catalysis enabled by Sm^{III}-alkoxide Protonolysis. *Science* **2024**, *385* (6711), 847−853.

(24) Chan, A. Y.; Perry, I. B.; Bissonnette, N. B.; Buksh, B. F.; Edwards, G. A.; Frye, L. I.; Garry, O. L.; Lavagnino, M. N.; Li, B. X.; Liang, Y.; Mao, E.; Millet, A.; Oakley, J. V.; Reed, N. L.; Sakai, H. A.; Seath, C. P.; MacMillan, D. W. C. Metallaphotoredox: The Merger of Photoredox and Transition Metal Catalysis. *Chem. Rev.* **2022**, *122* (2), 1485−1542.

(25) Meyer, A. U.; Slanina, T.; Heckel, A.; König, B. Lanthanide Ions Coupled with Photoinduced Electron Transfer Generate Strong Reduction Potentials from Visible Light. *Chem.—Eur. J.* **2017**, *23* (33), 7900−7904.

(26) Jenks, T. C.; Bailey, M. D.; Hovey, J. L.; Fernando, S.; Basnayake, G.; Cross, M. E.; Li, W.; Allen, M. J. First Use of a Divalent Lanthanide for Visible-Light-Promoted Photoredox Catalysis. *Chem. Sci.* **2018**, *9* (5), 1273−1278.

(27) Tomar, M.; Bhimpuria, R.; Kocsi, D.; Thapper, A.; Borbas, K. E. Photocatalytic Generation of Divalent Lanthanide Reducing Agents. *J. Am. Chem. Soc.* **2023**, *145* (41), 22555−22562.

(28) Kuribara, T.; Kaneki, A.; Matsuda, Y.; Nemoto, T. Visible-Light-Antenna Ligand-Enabled Samarium-Catalyzed Reductive Transformations. *J. Am. Chem. Soc.* **2024**, *146* (30), 20904−20912.

(29) Yoon, T. P. Photochemical Stereocontrol Using Tandem Photoredox-Chiral Lewis Acid Catalysis. *Acc. Chem. Res.* **2016**, *49* (10), 2307−2315.

(30) Huang, X.; Luo, S.; Burghaus, O.; Webster, R. D.; Harms, K.; Meggers, E. Combining the Catalytic Enantioselective Reaction of

Visible-Light-Generated Radicals with a by-Product Utilization System. *Chem. Sci.* **2017**, *8* (10), 7126−7131.
(31) Jung, J.; Kim, J.; Park, G.; You, Y.; Cho, E. J. Selective Debromination and α-Hydroxylation of α-Bromo Ketones Using Hantzsch Esters as Photoreductants. *Adv. Synth. Catal.* **2016**, *358* (1), 74−80.
(32) Ohnishi, Y.; Kagami, M.; Ohno, A. Reduction by a Model of NAD(P)H. Photo-Activation of NADH and Its Model Compounds toward the Reduction of Olefins. *Chem. Lett.* **1975**, *4* (2), 125−128.
(33) Johansen, C. M.; Boyd, E. A.; Peters, J. C. Catalytic Transfer Hydrogenation of N_2 to NH_3 via a Photoredox Catalysis Strategy. *Science Advances* **2022**, *8* (43), eade3510.
(34) Ji, C.-L.; Han, J.; Li, T.; Zhao, C.-G.; Zhu, C.; Xie, J. Photoinduced Gold-Catalyzed Divergent Dechloroalkylation of Gem-Dichloroalkanes. *Nat. Catal.* **2022**, *5* (12), 1098−1109.
(35) Liu, Y.; Lin, S.; Zhang, D.; Song, B.; Jin, Y.; Hao, E.; Shi, L. Photochemical Nozaki-Hiyama-Kishi Coupling Enabled by Excited Hantzsch Ester. *Org. Lett.* **2022**, *24* (18), 3331−3336.
(36) Pitre, S. P.; Allred, T. K.; Overman, L. E. Lewis Acid Activation of Fragment-Coupling Reactions of Tertiary Carbon Radicals Promoted by Visible-Light Irradiation of EDA Complexes. *Org. Lett.* **2021**, *23* (3), 1103−1106.
(37) Deng, G.; Xu, H.-J.; Chen, D.-W. Mechanism of Photoreduction of Diethyl Benzylidene Malonates by NAD(P)H Model and Comparison with Thermal Reaction. *J. Chem. Soc., Perkin Trans. 2* **1990**, *7*, 1133−1137.
(38) Slinker, J. D.; Gorodetsky, A. A.; Lowry, M. S.; Wang, J.; Parker, S.; Rohl, R.; Bernhard, S.; Malliaras, G. G. Efficient Yellow Electroluminescence from a Single Layer of a Cyclometalated Iridium Complex. *J. Am. Chem. Soc.* **2004**, *126* (9), 2763−2767.
(39) Shen, G.-B.; Fu, Y.-H.; Zhu, X.-Q. Thermodynamic Network Cards of Hantzsch Ester, Benzothiazoline, and Dihydrophenanthridine Releasing Two Hydrogen Atoms or Ions on 20 Elementary Steps. *J. Org. Chem.* **2020**, *85* (19), 12535−12543.
(40) Schmittel, M.; Burghart, A. Understanding Reactivity Patterns of Radical Cations. *Angew. Chem., Int. Ed.* **1997**, *36* (23), 2550−2589.
(41) Boyd, E. A.; Peters, J. C. Sm(II)-Mediated Proton-Coupled Electron Transfer: Quantifying Very Weak N-H and O-H Homolytic Bond Strengths and Factors Controlling Them. *J. Am. Chem. Soc.* **2022**, *144* (46), 21337−21346.
(42) Analogous net proton-coupled electron transfer to Ti(IV)-alkoxide species to generate Ti(III) has been proposed in photodriven Ti redox catalysis: Gualandi, A.; Calogero, F.; Mazzarini, M.; Guazzi, S.; Fermi, A.; Bergamini, G.; Cozzi, P. G. Cp_2TiCl_2-Catalyzed Photoredox Allylation of Aldehydes with Visible Light. *ACS Catal.* **2020**, *10* (6), 3857−3863.
(43) Chciuk, T. V.; Flowers, R. A. Proton-coupled Electron Transfer in the Reduction of Arenes by SmI_2-water Complexes. *J. Am. Chem. Soc.* **2015**, *137* (35), 11526−11531.
(44) Kolmar, S. S.; Mayer, J. M. $SmI_2(H_2O)_n$ Reduction of Electron Rich Enamines by Proton-coupled Electron Transfer. *J. Am. Chem. Soc.* **2017**, *139* (31), 10687−10692.
(45) Boekell, N. G.; Bartulovich, C. O.; Maity, S.; Flowers, R. A. I. Accessing Unusual Reactivity through Chelation-Promoted Bond Weakening. *Inorg. Chem.* **2023**, *62* (12), 5040−5045.
(46) Kern, N.; Plesniak, M. P.; McDouall, J. J. W.; Procter, D. J. Enantioselective Cyclizations and Cyclization Cascades of Samarium Ketyl Radicals. *Nat. Chem.* **2017**, *9* (12), 1198−1204.
(47) Evans, D. A.; Nelson, S. G.; Gagne, M. R.; Muci, A. R. A Chiral Samarium-Based Catalyst for the Asymmetric Meerwein-Ponndorf-Verley Reduction. *J. Am. Chem. Soc.* **1993**, *115* (21), 9800−9801.
(48) Wang, Y.; Zhang, W.-Y.; Yu, Z.-L.; Zheng, C.; You, S.-L. SmI_2-Mediated Enantioselective Reductive Dearomatization of Non-Activated Arenes. *Nat. Synth* **2022**, *1* (5), 401−406.
(49) Miller, R. S.; Sealy, J. M.; Shabangi, M.; Kuhlman, M. L.; Fuchs, J. R.; Flowers, R. A. Reactions of SmI_2 with Alkyl Halides and Ketones: Inner-Sphere vs Outer-Sphere Electron Transfer in Reactions of Sm(II) Reductants. *J. Am. Chem. Soc.* **2000**, *122* (32), 7718−7722.
(50) Speckmeier, E.; Fischer, T. G.; Zeitler, K. A Toolbox Approach To Construct Broadly Applicable Metal-Free Catalysts for Photoredox Chemistry: Deliberate Tuning of Redox Potentials and Importance of Halogens in Donor-Acceptor Cyanoarenes. *J. Am. Chem. Soc.* **2018**, *140* (45), 15353−15365.
(51) Mikami, K.; Yamaoka, M. Chiral Ligand Control in Enantioselective Reduction of Ketones by SmI_2 for Ketyl Radical Addition to Olefins. *Tetrahedron Lett.* **1998**, *39* (25), 4501−4504.
(52) CV experiments suggest that speciation of 1:1 SmI_3:BINAPO is a complex mixture with $Sm^{III/II}$ redox waves negative of −2 V (Figure S43).
(53) Substrate coupling could be initiated either by ketone or acrylate reduction, leading to either an α-ester radical or an alkoxy radical intermediate, respectively, following addition to the corresponding coupling partner. In the case of difficult-to-reduce ketone substrates such as **1**, neither pathway can be reliably ruled out. See the following and ref 54 for detailed examination of this mechanistic question: Hansen, A. M.; Lindsay, K. B.; Sudhadevi Antharjanam, P. K.; Karaffa, J.; Daasbjerg, K.; Flowers, R. A.; Skrydstrup, T. Mechanistic Evidence for Intermolecular Radical Carbonyl Additions Promoted by Samarium Diiodide. *J. Am. Chem. Soc.* **2006**, *128* (30), 9616−9617.
(54) Sono, M.; Hanamura, S.; Furumaki, M.; Murai, H.; Tori, M. First Direct Evidence of Radical Intermediates in Samarium Diiodide Induced Cyclization by ESR Spectra. *Org. Lett.* **2011**, *13* (21), 5720−5723.

https://doi.org/10.1021/jacs.4c10053
J. Am. Chem. Soc. 2024, 146, 25456−25461